1. Miloudi Khaled, 2. Sellami Mabrouk, 3. Allaoui Tayeb, 4.Boukhlif Rafik, 5. Denai Mouloud5

[1,2]Laboratory of Energetic Engineering : Team SIMULA ENARGARIDTahri Mohamed University, Bechar, Algeria
[3]Laboratory of Energetic Engineering and Computer Engineering, Ibn Khaldoun University, Tiaret, Algeria,
[4]Automation, Vision and Intelligent Control of Systems, USTO, Oran, Algeria.
[5] Prof., School of Engineering and Computer Science, University of Hertfordshire, Hatfield, UK,
ORCIG.

doi:10.15199/48.2021.12.02

Performance enhancement of a solar water pumping system using a new three level parallel multicellular converter topology

Abstract. *The use of phtovoltaic energy in water pumping is an economically viable and sustainable solution to rural communities without access to the electricity grid. The aim of this paper is to improve the performance of a phtovoltaic water pumping system by using a new converter structure based on three levels parallel multicell converter. This converter is controlled by two control loops, an external control based on the SMC and FLC MPPT algorithms and an internal control of the output branch current with the hybrid control based on the Petri nets. A comparative study between the boost converter and a three-levels parallel multicellular converter with the SMC and FLC MPPT has been made, which allows us to conclude that the new structure is more advantageous than the conventional structure especially. The boost gives rise to a wide band of strong power oscillations as well as the current and a voltage of PV, which translates into a high harmonic ratio with respect to the three-level parallel multicellular converter structure.*

Streszczenie. *Wykorzystanie energii fotowoltaicznej do pompowania wody jest ekonomicznie opłacalnym i zrównoważonym rozwiązaniem dla społeczności wiejskich bez dostępu do sieci elektrycznej. Celem tego artykułu jest poprawa wydajności fotowoltaicznego systemu pompowania wody poprzez zastosowanie nowej struktury konwertera opartej na trójpoziomowym równoległym konwerterze wieloogniwowym. Przetwornica ta jest sterowana przez dwie pętle sterowania, sterowanie zewnętrzne oparte na algorytmach SMC i FLC MPPT oraz sterowanie wewnętrzne prądu gałęzi wyjściowego ze sterowaniem hybrydowym opartym na sieciach Petriego. Przeprowadzono badanie porównawcze pomiędzy konwerterem boost a trójpoziomowym równoległym konwerterem wielokomórkowym z SMC i FLC MPPT, co pozwala stwierdzić, że nowa konstrukcja jest szczególnie korzystniejsza niż konstrukcja konwencjonalna. Wzmocnienie powoduje powstanie szerokiego pasma silnych oscylacji mocy oraz prądu i napięcia PV, co przekłada się na wysoki współczynnik harmonicznych w stosunku do trójpoziomowej równoległej struktury wielokomórkowej przetwornic.* (***Poprawa wydajności solarnego systemu pompowania wody przy użyciu nowej trójpoziomowej równoległej topologii wielokomórkowej konwertera***)

Keywords: Water pumping Photovoltaic system, Petri nets, MPPT, Fuzzy Logic, Sliding mode, Boost converter, Multicellular converter
Słowa kluczowe: Pompowanie wody System fotowoltaiczny, sieci Petriego, MPPT, Fuzzy Logic, tryb ślizgowy, konwerter Boost..

1.Introduction

Solar photovoltaic-powered pumping systems have now become a mature and economically attractive technology for rural and isolated communities water supply and agriculture applications.

In recent years, there has been extensive research to improve the performance of photovoltaic pumping systems. The first studies in this type of systems based on DC motors, in [01] the author focuses on the characteristics of the MCC powered by solar cells. In [02] the author analyzes the start of a photovoltaic pumping system powered by solar modules with and without MPPT regulator. In [03,04] the author studies the operation of a MCC with a converter elevator "Boost" and a MPPT regulator. In [05,06,07], the authors studied optimization photovoltaic pumping system.
The design of a power conversion stage now makes it easy to connect a photovoltaic generator with a DC load with a very high conversion efficiency. In fact, the concept of this floor corresponds to modeling the idealized basic functions of a switching converter continuous-DC (DC / DC) [08]. To extract, at every moment, the maximum of power available at the terminals of the GPV and transfer it to the load, a stage adaptation is used. This stage acts as an interface between the two elements. It ensures, through a control action, the transfer of maximum power provided by the generator. The adapter commonly used in photovoltaics is a static converter (DC / DC power converter). The structure conversion is chosen according to the load to feed. She may be revolving or devolving. [09]

The conventional converters used for several decades, we group under the name of conventional converters 2-level and 3-level converters. With a power of a few kVA to a hundred MVA, they are technologically proven and are present in most industrial applications proposed by major manufacturers [10] such as photovoltaic power generation. They have the following advantages:

The number of components is reduced (minimum for the 2-level inverter) and requires one to two voltage sources at maximum,

The numerous modulation strategies make it possible to optimize the use of these converters and offer a certain flexibility of the control / command part,

- The switching frequency can be high at low power and can reach several tens of kHz for applications requiring fast current control.

And disadvantages:

The amplitude of the output voltage level depends on the voltage withstand of the components used. For a higher voltage level, serialization of components is inevitable,

The THD of the output voltage of the converter is important. It reaches about 60% for a 2-level converter and 30% for a 3-level converter. Generally, a harmonic filtering at the output of the converter is necessary,

The switching frequency is very quickly limited for high power converters because of the losses generated in the components. It is of the order of kHz [09].
From a historical point of view, the emergence of multilevel converters based on power components such as thyristors and transistors starts from the 1960s [11]. The first structure described is a series connection of H-bridge and then in the late 1970s appeared the neutral clamped converter (NPC), this structure is considered the first multilevel converter for medium power applications. Since then, numerous studies have been proposed to study its properties and the possible evolutions of this structure. In the 90s, research into new structures was carried out to the multicellular series converters, also known in the literature as Flying Capacitor (FC), and it was in the late 1990s that the Multicellular converter superimposed, this structure is a continuation of the reflection on serial multicell converters. These structures can be considered as the basic structures of multilevel conversion [12].

The paper is organized as follows: The description and a model of the PV system are presented in Section 2. In Section 3, modeling of BOOST and three levels multicellular parallel converters. A maximum power point tracking (MPPT) control using P&O, sliding mode and fuzzy logic techniques are presented in Section 4. The internal control of the three levels parallel multicellular converter is developed and explained in Section 5.The simulation results are presented in Section 6 and finally discussions and conclusions are given in Section 7.

2. Configuration and modeling of the solar water pumping system

The photovoltaic pumping system considered in this study is depicted in Fig. 1. It consists of PV array, a motor pump based on an induction motor with an adaptation between the source and the load. The motor pump is driven by a three-level parallel multicellular converter and an inverter.

To improve the efficiency of the PV system, a Maximum Power Point Maximum Power Point Tracker (MPPT).

The overall system was simulated in MATLAB/Simulink to validate the effectiveness of the proposed control strategy.

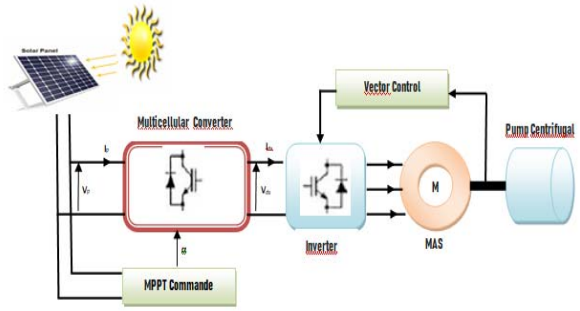

Fig.1. Configuration of a photovoltaic water pumping systembased a three levels multicellular converter

This paper presents a comprehensive comparative analysis of the boost converter and a three three levels parallel multicellular converter with a command MPPT for a photovoltaic water pumping system. The multicell converter requires an internal control; we will regulate it by the hybrid control based on the Petri nets provide. The results of the simulation show that the proposed design approach is effective in finding optimal controller parameters and thereby improving the transient performance of PV system over a wide range of operating conditions.

2.1 Modeling of the PV Array

The electric power generated from the PV array fluctuates with the operating conditions and field factors such as the sun's position angle, irradiation levels and ambient temperature. A solar cell can be represented as a current source model as shown in Fig. 2.

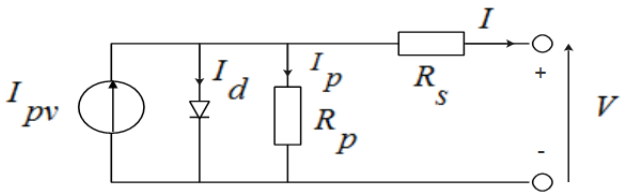

Fig.2. Single-diode equivalent circuit of a pv cell

Applying Kirchhoff's current law, the terminal current of the cell is:

$$I = I_{pv} - I_d - I_p \tag{1}$$

$$I_p = \frac{V + R_s I}{R_p} \tag{2}$$

The junction current is given by:

$$I_d = I_0 \left[e^{\left(\frac{V + R_s I}{V_t \alpha} \right)} - 1 \right] \tag{3}$$

The formula relating the current and voltage in the circuit is:

$$I = I_{pv} - I_0 \left[e^{\left(\frac{V + R_s I}{V_t \alpha} \right)} - 1 \right] - \frac{V + R_s I}{R_p} \tag{4}$$

$$V_t = \frac{N_s K T}{q} \tag{5}$$

The light generated current of the PV cell depends linearly on the solar irradiation and is also dependent on the temperature according to the following equation [12], [13]:

$$I_{pv} = \left(I_{pv,n} + K_I \Delta_T \right) + \frac{G}{G_n} \tag{6}$$

The diode saturation current and its dependence on the temperature may be expressed by:

$$I_0 = \frac{I_{sc,n} + K_I \Delta_T}{\left(\frac{I_{oc,n} + K_V \Delta_T}{\alpha V_t} \right) - 1} \tag{7}$$

The parameters and model constants of the KC200GT solar array, used in this study,are given in the Appendix.

2.2 Modeling of a three -levels parallel converters

The 3 levels parallel multicell converter is a power converter for achieving an output current equal to n times the input current figure 3 [14].

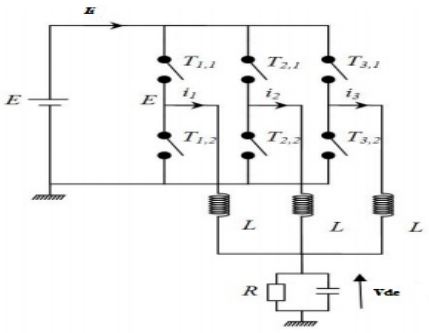

Fig.3. A three 3-cell parallel multicellular converter.

Depending on the number of cells and the state of the switches S, the parallel multicellular can be modeled by the following system of equations:

$$L \frac{di_1}{dt} = -R_L i_1 - vc + s_1 E \tag{8}$$

$$L \frac{di_P}{dt} = -R_L i_P - vc + s_P E \tag{9}$$

$$C \frac{dv_C}{dt} = i_1 + \cdots i_P - \frac{v_C}{R} \tag{10}$$

with p the number of cells, ik, k = 1, .., p the current flowing in the kth branch, vC the output voltage and sk the kth

command such that its value is expressed by the following function:

$$s_K(t)=\begin{cases} 1, & S_{on} \\ 0, & S_{off} \end{cases}$$

3. Maximum power tracking and control strategies

Fig. 4 shows the basic circuit configuration of a DC-DC boost converter with an MPPT controller. A capacitor is generally connected between the PV panel and the boost circuit to reduce high frequency harmonics [06], [07].

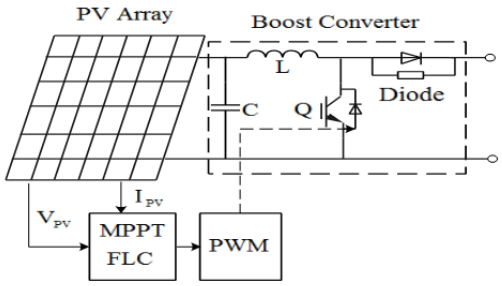

Fig.4. System based a boost converter and mppt control.

Fig. 5 shows the basic circuit configuration of a DC-DC a parallel multicellular converter with an MPPT controller.

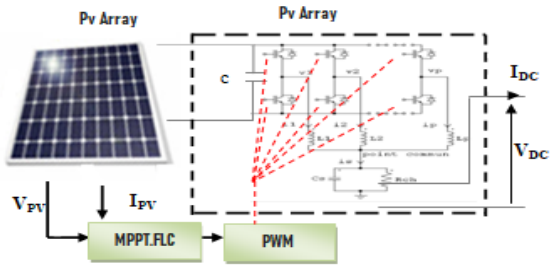

Fig.5. PV system based a parallel multicellular converter and MPPT control.

3.1 Mppt based on fuzzy logic

This control strategy consists of three main building block: Fuzification, Fuzzy Inference and Defuzification treat two input, the error ΔP/Δv, the change of error d(ΔP/Δv) for varied the duty cycle D which drives the static converter to look for the PPM [13].

Similar FLC-based MPPT controllers have been proposed in the basic structure of a FLC is shown in Fig. 6. The inputs are the error E and error change dE; the output is the PWM duty cycle variation dD.

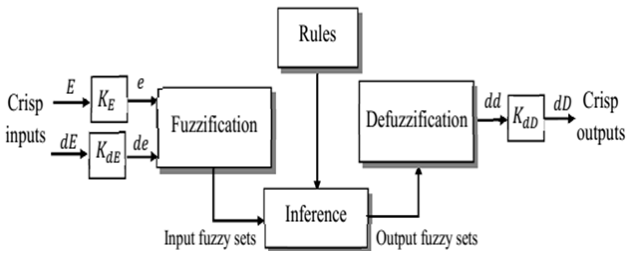

Fig.6. MPPT based on FLC.

where KE, KdE and KdD are scaling gains selected to achieve the desired transient and steady-state response characteristics [06,07]. The universe of discourse for each input and output variable is divided into five fuzzy sets defined by triangular membership functions and labelled as NB (Negative Big), NS (Negative Small), ZE (Zero), PS (Positive Small) et PB (Positive Big) as shown in Fig.7. The fuzzy rules used to determine the controller output are summarized in Table 1. The defuzzificationis based on the popular centre of gravity method.

Table 1.Fuzzy control rules.

Dp/Dv CE	NB	NS	ZE	PS	PB
NB	ZE	ZE	PS	NS	NB
NS	ZE	ZE	ZE	NS	NB
ZE	PB	PS	ZE	NS	NB
PS	PB	PS	ZE	ZE	ZE
PB	PB	PS	NS	ZE	ZE

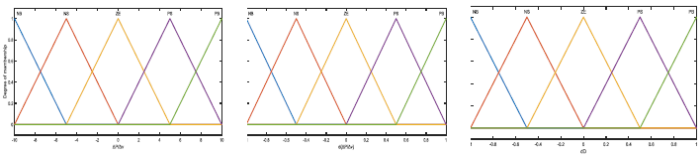

Fig.7. Fuzzy membership functions for the input and output variables.

3.2 Mppt based on sliding mode controller (SMC)

One must constitute a law of order as follows [14]:

$$U = U_{eq} + U_{slg} \quad (10)$$

$$U_{eq} = K\left(X - X_{ref}\right) \quad (11)$$

$$U_{slg} = K_{slg}.\mathrm{Sign(S(x))}. \quad (12)$$

Such as ; K: the gain by state feedback, Kslg: the slip gain, X: the state variable (the Ipvcurrent), Xref: the reference state variable (Ipvref), S (x): the surface sliding, Ueq: the equivalent part of the control law, Uslg: the sliding part of the law controls, SPCL: the sliding part of the control law, U: the control law.

The purpose of this command is to turn off the maximum power by canceling $\frac{D_p}{D_v}$. We have

$$P = V.I \rightarrow \frac{D_p}{D_v} = I.\frac{D_v}{D_v} + v.\frac{D_i}{D_v} \quad (13)$$

$$\frac{D_p}{D_v} = I + v.\frac{D_i}{D_v} \quad (14)$$

$$(S(x) = \frac{D_p}{D_v}) \quad (15)$$

$$S(x) = 0 \rightarrow \frac{D_p}{D_v} = I_{ref} + V.D\frac{D_{I_{PV}}}{D_{V_{PV}}} = 0 \rightarrow I_{ref} = -V_{PV}\frac{D_{I_{PV}}}{D_{V_{PV}}} \quad (16)$$

when

$$\frac{D_p}{D_v} = I + V_{PV}\frac{D_{IPV}}{D_{V_{PV}}} = I_{PV} - I_{PVref} \quad (17)$$

$$\mathrm{S(x)} = I_{PV} - I_{PVref} = X - X_{ref} \quad (18)$$

Finally the control law is modeled by the following equations:

$$U = U_{eq} + U_{slg} \quad (19)$$

$$U_{eq} = K(I_{PV} - I_{PV}ref) \quad (20)$$

$$U_{slg} = K_{slg}.Sing\,(U_{slg} = K_{slg}.Sing(I_{PV} - I_{PVref}) \quad (21)$$

After modeling this command is presented by the block diagram – Fig. 8.

To have a good functioning of our system we can see the best results by the gain of return of state and the gain of slip.

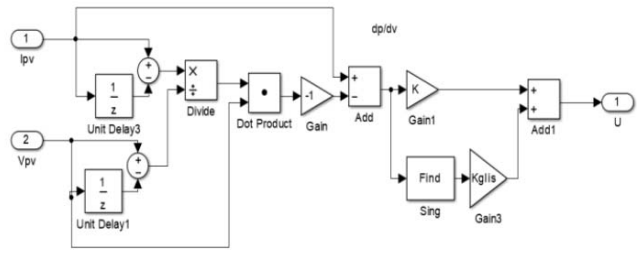

Fig.8. Block diagram of the MPPT based sliding mode control

4.Controllers schemes for the three-level multicellular converter

In this section, the hybrid control of the parallel multicellular converter based on the Petri nets are developed for a three levels multicellular power converter.

4.1. Hybrid control of the parallel multicellular converter based on the Petri nets

Petri Dynamic systems are usually continuous or discrete or both.In our case we have, an SDH has two subassemblies a continuous block and a discrete block [15]: the continuous block symbolizes the dynamic evolution of the continuous state in our case the link inductances, the output capacity and the load.

the discrete block presents the system with discrete event it receives events of the cells of commutation.

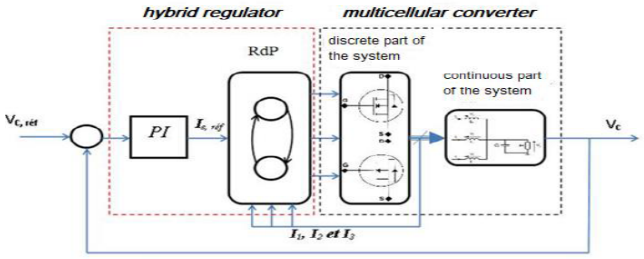

Fig.9. The diagram representing the hybrid control of the multicellular converter [15]

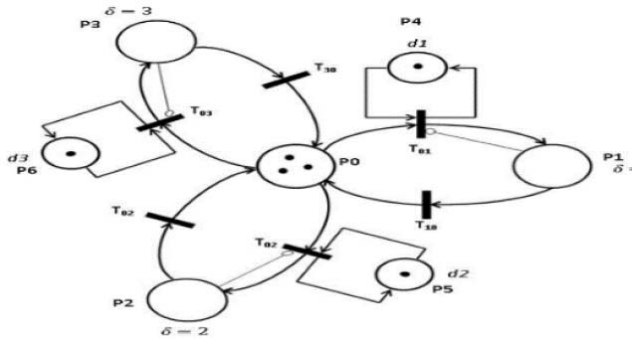

Fig.10. The RDP of the switch control of the 3-cell switch converters [15]

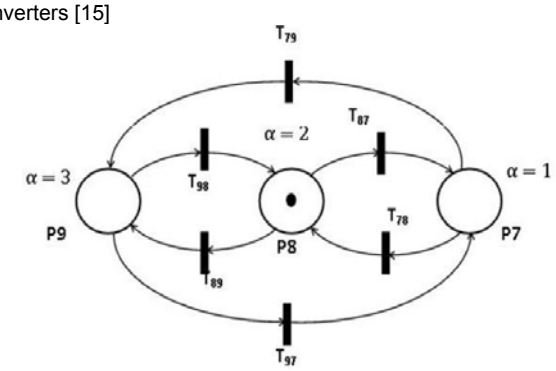

Fig.11. Petri net of possible configurations [15].

This command contains two parts, a continuous part and a discrete one, the first is based a PI regulator ensuring the regulation of the output voltage, the second control loop is modeled by a RAP where the latter poses a regulation of the current Is to the Isref value calculated by the PI.

This current regulation is followed by a balancing of branch currents to ensure a better distribution of the latter in each branch [15], [16]. The RDP of the switch control is represented by the figures 10 and 11.

4.2. Describing the possible configurations of the converter

Pi: places, i = 0 ... ..9, Tij: the transition from place i to place j; j = 0 ... ..9, αi: the configuration; i = 1,2,3, di: the residence time we chose d1 = d2 = d3.

The figure 12 gives the three possible cases of the converter configuration.

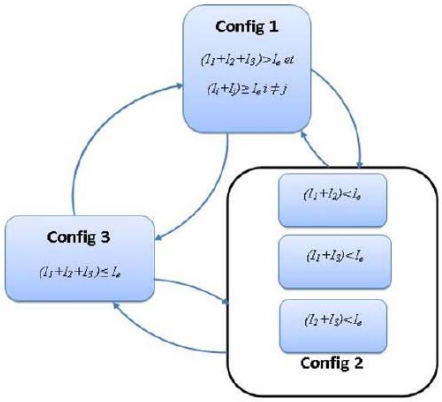

Fig.12. The allowed configurations according to currents I1, I2, i3 and Ie [15].

The meaning of all places and transitions is shown in the table 03 with Min1 = min (I1, I2, I3), min2 = min ((I1 + I2), (I1 + I3), (I2 + I3)) and Iref = Isref / 3.

Table2.Signification of places [15].

Seats	Designations
P_0	initial state
P_1	states of the switch of the 1st cell
P_2	states of the switch of the 2nd cell
P_3	states of the switch of the 3rd cell
P4, P5 , P_6	timed places designating the allowed time between two commutations of a switch
P_7	Config 1 only one switch is allowed to be closed
P_8	Config 2 two switches are allowed to be closed
P_9	Config 3 three switches are allowed to be closed

Table3.Transitions [15].

Transitions	Designations
T_{01}	$I1 < Iref and\ [\alpha = 3\ or\ \{(\alpha = 2) and \begin{bmatrix}(I1+I2) = min2\ and \delta \neq 3\\ or(I1+I3) = min2\ and \delta \neq 2\end{bmatrix} or\{\alpha = 1\ and I1 = min1\ and \delta \neq 2\ and \delta \neq 3\}\}]$
T_{02}	$I2 < Iref and\ [\alpha = 3\ or\ \{(\alpha = 2) and \begin{bmatrix}(I1+I2) = min2\ and \delta \neq 3\\ or(I1+I3) = min2\ and \delta \neq 2\end{bmatrix} or\{\alpha = 1\ and I1 = min1\ and \delta \neq 2\ and \delta \neq 3\}\}]$
T_{03}	$I3 < Iref and\ [\alpha = 3\ or\ \{(\alpha = 2) and \begin{bmatrix}(I1+I3) = min2\ and \delta \neq 2\\ or(I2+I3) = min2\ and \delta \neq 1\end{bmatrix} or\{\alpha = 1\ and I3 = min1\ and \delta \neq 2\ and \delta \neq 1\}\}]$

T_{20}	$I2 \geq Ieor[(I1+I2+I3) \geq Ie]or[(I2+Ik) = min2+\Delta2]or[I2 \geq min1+\Delta1]$
T_{30}	$I3 \geq Ieor[(I1+I2+I3) \geq Ie]or[(I3+Ik) = min2+\Delta2]or[I3 \geq min1+\Delta1]$
T_{87}, T_{97}	$[(Ii+Ij) > Iei \neq j]$
T_{78}, T_{98}	$[(I1+I2+I3) > Ie]$ and $[(I1+Ij) < Iei \neq j]$
T_{89}, T_{79}	$[(I1+I2+I3) \leq Ie]$

The imbalance of the phase currents and one of the major problems of this type of converter, this imbalance causes a failure on the voltage source if one of the branch currents will exceed the authorized current input.

5. Simulation resultats and discution

In this section, we will first present the simulation results of photovoltaic system based on the boost and the parallel multicellular converter and secondly we will present the results of the photovoltaic water pumping system based on the three levels parallel multicellular converter.

5.1. PV water pumping system based on the boost and the parallel multicellular converter

In order to demonstrate the advantage of the three-levels parallel multicellular converter compared to the simple boost converter, we present in this part the results obtained for the two structures with the SMC and FLC MPPT.

The PV conversion system and MPPT control schemes studied are simulated in Matlab/Simulink and SimpowerSystem toolbox with the parameters given in the Appendix. This simulation study will be based on constant weather conditions (T= 25°C and R = 1000 W/m2).

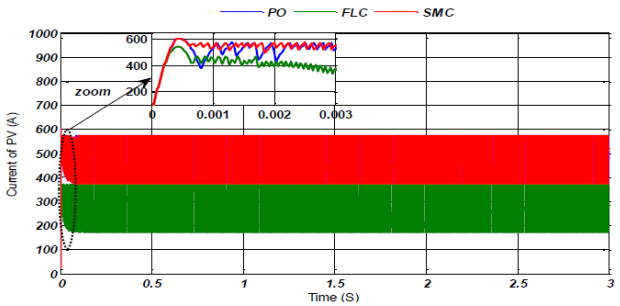

Fig.13.PV current with a boost converter.

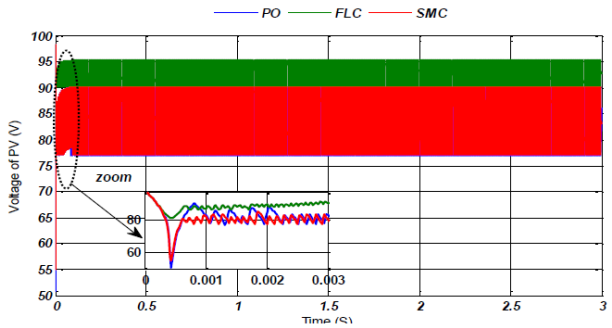

Fig.14.PV voltage with a boost converter

The figures 13 through 15present the PV characteristics with a boost converter and the figures 16 through 18 present the PV characteristics with a three parallel multicellular converter. These figures show that the photovoltaic system is converging towards optimal values. The P & O algorithm is a classic and simple algorithm. In general, this algorithm strongly depends on the initial conditions and it presents oscillations around the optimal value. Therefore, this method seem just an approximation, they do not have enough precision, and then the system does not always work at the optimal point. The fuzzy logic and sliding mode algorithms are a robust and efficient algorithm. Indeed, these algorithms works at the optimal point without oscillations. In addition, it is characterized by good transient behavior. However, the implementation of this type of algorithm is more complex than conventional algorithms.

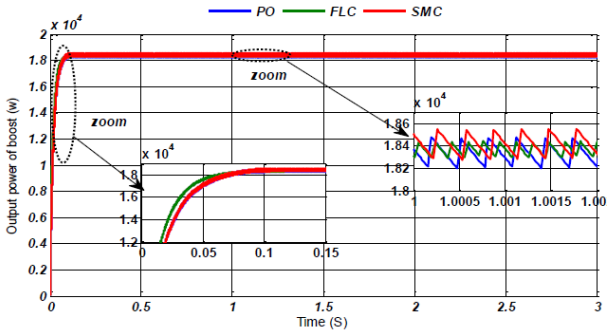

Fig.15.Power of PV with a boost converter.

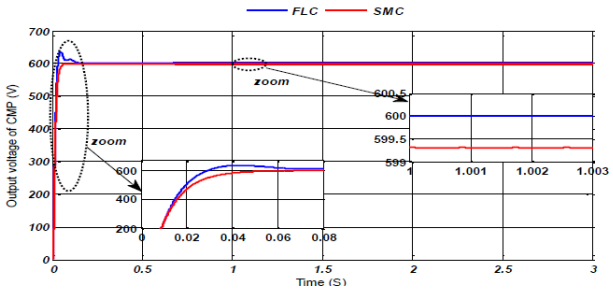

Fig.16. PVvoltage with a three parallel multicellular converter.

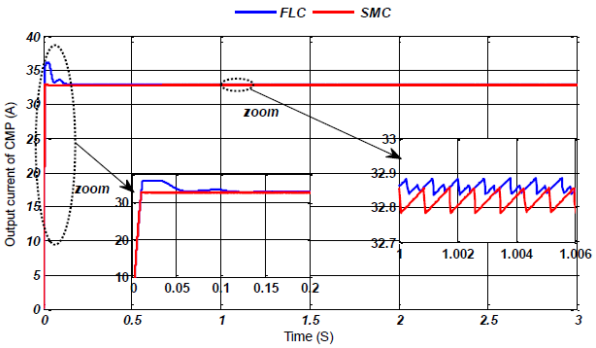

Fig.17. PV current with a three parallel multicellular converter.

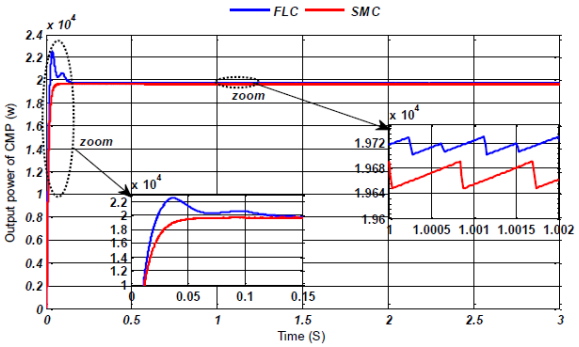

Fig.18. Power of PV with a three parallel multicellular converter.

A comparative study between the boost converter and three-level parallel multicellular converter with the SMC and FLC-MPPT has been made, which allows us to conclude that the new structure is more advantageous than the conventional structure especially. The boost gives rise to a wide band of strong power oscillations as well as the

current and a voltage of PV, which translates into a high harmonic ratio with respect to the three-level parallel multicellular converter structure.

5.2. PV water pumping system based on the three levels parallel multicellular converter.

It should be mentioned that the parallel multicellular converter in this structure is controlled by two control loops, an external control based on the FLC MPPT algorithm, and an internal control of the output branch current with the hybrid control based on the Petri nets.

Figures 19, 20 and 21 respectively show the current, the voltage and the power supplied by the PV. We can well see that the power follows its optimal value (45250W) with small ripples.

Figure 22 show the evolutions of the floating voltages of the three levels parallel multicellular converter controlled by Petri Nets. We observe that the floating voltage reaches their reference. The error is greatly attenuated with a low rate of the order of 0.5%. The major advantage of this command is its range of validity. Indeed, it has shown its effectiveness for different reference values. This figure show that the proposed control strategy is effective and leads to satisfactory results and consistent objectives.

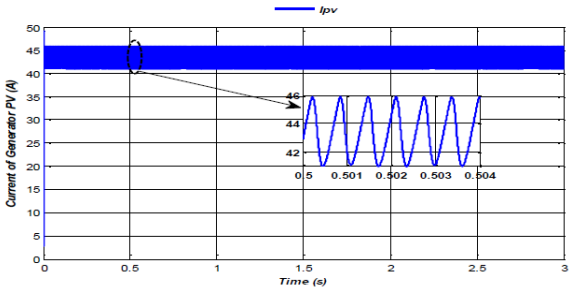

Fig.19. PV current in photovoltaic water pumping system.

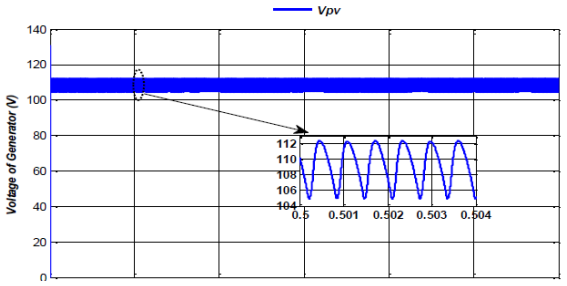

Fig.20. PV voltage in photovoltaic water pumping system

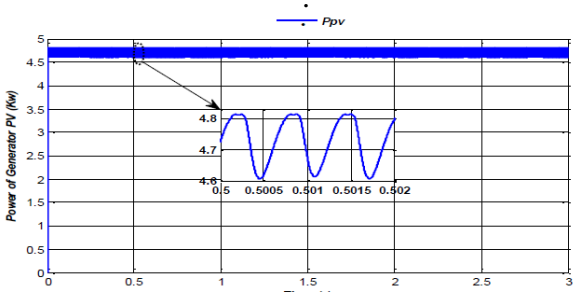

Fig.21.power of PV in photovoltaic water pumping system

The figures 23 through 26 show the magnitudes of the motor which drives the pump, the stator current, stator voltage, rotational speed and mechanical torque. As depicted from these figures, the proposed control strategy “Petri Nets” has a better and enhanced response. The oscillations in the system states have been considerably reduced for the proposed three-level parallel multicellular converter topology as compared to BOOST converter.

Figure 25 show the evolutions of the mechanical torque, we observe that this last reaches their reference.

It is observed that the speed of rotation is totally confused with its reference speed after a very short time.

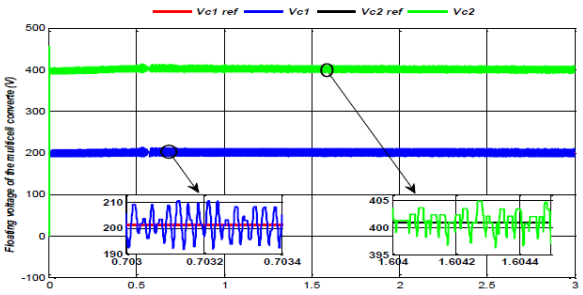

Fig.22. Floating voltage of the three levels parallel multicellular converter

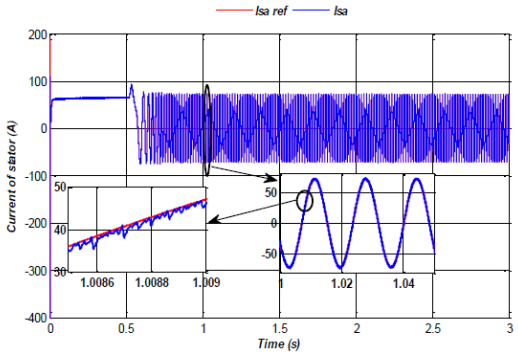

Fig.23. Statorique current of an induction motor.

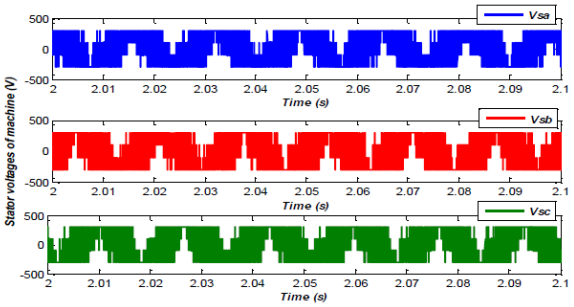

Fig.24. Statorique voltage of an induction motor.

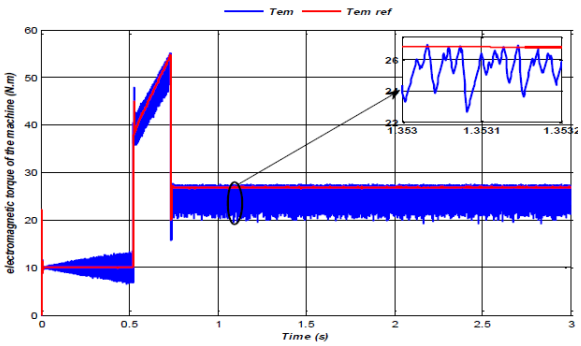

Fig.25. Electromagnetic torque of an induction motor.

The figures 27, 28 and 29 respectively show the power of the pump, the height of the pumped water and the flow of water.

It can be seen that the pumping PV system results based on the multicellular converter have curves with fewer ripples compared to those obtained by the same system based on the boost converter.

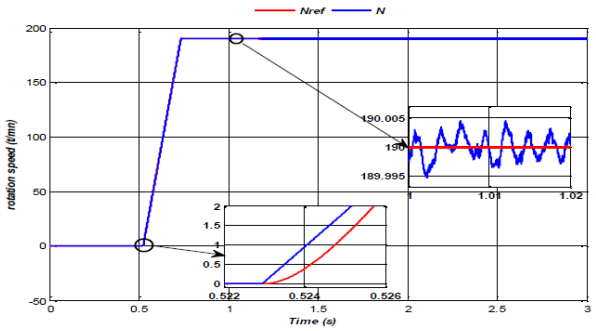

Fig.26. Rotation speed.

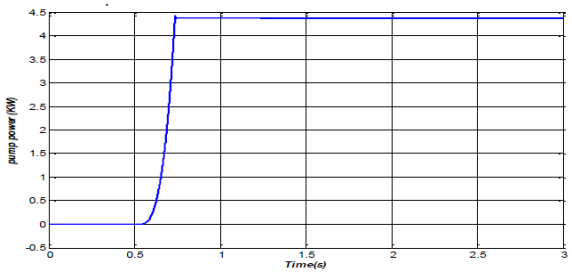

Fig.27. Pump power.

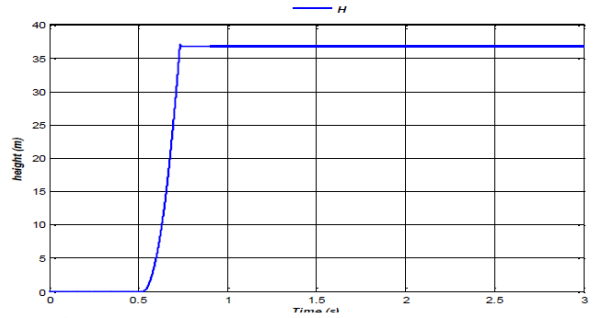

Fig.28. Height power.

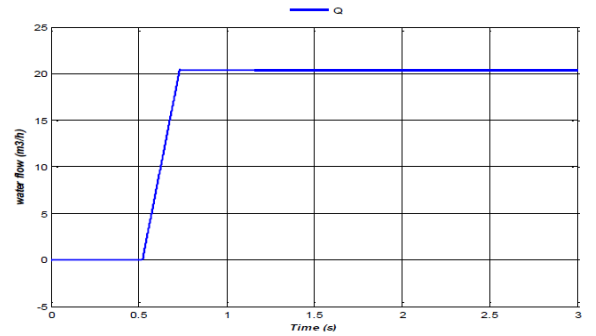

Fig.29. Water flow.

6. Conclusions

In this paper article a new contribution in the application of multicellular converter as adaptation stage in aa photovoltaic pumping system with field oriented control (FOC).The simulation results show that the control with an internal control of the output branch current with the hybrid control based on the Petri nets is more efficient in terms of stability, precision and speed to reach the maximum power point.

A comparative study between the boost converter and three-level parallel multicellular converter with the SMC and FLC MPPT has been made, which allows us to conclude that the new structure is more advantageous than the conventional structure especially. The boost gives rise to a wide band of strong power oscillations as well as the current and a voltage of PV, which translates into a high harmonic ratio with respect to the three-level parallel multicellular converter structure.

A three MPPT algorithms (PO, SMC, FLC,) has been evaluated for tracking MPPs of a PV system for both structures. The simulation results show that improved performance has been achieved by these algorithms as compared to P&O. P&O method can cause large ondulationcaused by discontinuous control law and a of the parametrs system are actually known. SMC, FLC methods provides better performance and robustness even under large temperature and irradiation changes

REFERENCES

[1] Elgendy, M. A., Zahawi, B., and Atkinson, D. J., “Comparison of directly connected and constant voltage controlled photovoltaic pumping systems,” IEEE Trans. Sustain. Energy, Vol. 1, No. 3, pp. 184–192, October 2010.

[2] Raju, A. B., Ramesh Karnik, S., and Jyoti, R., “Maximum efficiency operation of a single stage inverter fed induction motor PV water pumping system,” First International Conference on Emerging Trends in Engineering and Technology, pp. 905–910, Nagur, India, 16– 18 July 2008.

[3] Chandrasekaran, N, Ganeshprabu, G, and Thyagarajah, K., “Comparative study of photovoltaic pumping system using a DC motor and PMDC motor,” International Conference on Advances in Engineering, Science and Management (ICAESM), pp. 192–132, Nagapattinam, India, March 2012.

[4] F.A.O. Aashoor et F. V. P. Robinson, « Maximum power point tracking of photovoltaic water pumping system using fuzzy logic controller », in Power Engineering Conference (UPEC), 2013 48th International Universities’, 2013, p. 1–5.

[5] A. M. Sharaf and Liang Yang, “A Novel Maximum Power Tracking Controller for a Stand-alone Photovoltaic DC Motor Drive” IEEE CCECE/CCGEI, Ottawa, May 2006.

[6] B. Belabbas, T. Allaoui, M. Tadjine, et M. Denai, « Power management and control strategies for off-grid hybrid power systems with renewable energies and storage », Energy Syst., p. 1–30, 2017.

[7] B. Belabbas, T. Allaoui, M. Tadjine, et M. Denai, « Power Quality Enhancement in Hybrid Photovoltaic-Battery System based on three–Level Inverter associated with DC bus Voltage Control », J. Power Technol., vol. 97, no 4, p. 272–282, 2017.

[8] Dylan D.C. Lu and Quang Ngoc Nguyen, “A Photovoltaic Panel Emulator Using A Buck-Boost DC/DC Converter and A Low Cost Micro-Controller,” Solar Energy, vol.86,no.5, pp.1477-1484, May 2012.

[9] B.Bai, C.Mi, andS.Gargies,“The short-time-scaletransient processes in highvoltage and highpower is olatedbidirectional DC-DC converters,”IEEETrans. Power Electron.

[10] GE, ABB, Siemens, Ansaldo, Schneider Electric, TMEIC, Rockwell, Mitsubishi Electric.

[11] Alexandre Leredde « Etude, commande et mise en oeuvre de nouvelles structures multiniveaux »,thése doctorat de l’université de toulouse novembre 2011.

[12] Mathieu Morati « Contribution à l’étude et au contrôle des convertisseurs multiniveaux : application à la compensation des fours à arc », thèse doctorat de l’université de lorraine juin 2014.

[13] H. E. A. Ibrahim et M. Ibrahim, « Comparison Between Fuzzy and P&O Control for MPPT for Photovoltaic System Using Boost Converter », J. Energy Technol. Policy, vol. 2, no 6, p. 1–11, 2012

[14]B. Yang et al., « Perturbation observer based fractional-order sliding-mode controller for MPPT of grid-connected PV inverters: Design and real-time implementation », Control Eng. Pract., vol. 79, p. 105–125, 2018.

[15]Bilal Amghar, MoumenDarcherif, Jean-Pierre Barbot, Patrick Gauthier. Modeling and control of parallel multicell chopper using Petri nets. 8th Power Plant and Power System Control Symposium - PPPSC 2012, Sep 2012, Toulouse, France.

[16]Drighiciu ” Application du formalisme réseaux de pétri pour la modélisation de systèmes hybrides” ICCPS (2007), Moldova pp. 152-155.